The Journal of Chemical Physics ARTICLE pubs.aip.org/aip/jcp

Calculating excitonic interactions using transition currents with application to PTCDA

Cite as: J. Chem. Phys. 163, 224127 (2025); doi: 10.1063/5.0297044
Submitted: 17 August 2025 • Accepted: 12 November 2025 •
Published Online: 11 December 2025

Grace Hsiao-Han Chuang,[1,a)] Ulf Saalmann,[1] and Alexander Eisfeld[1,2,b)]

AFFILIATIONS

[1] Max Planck Institute for the Physics of Complex Systems, Nöthnitzer Str. 38, 01187 Dresden, Germany
[2] Institute of Theoretical Physics, TUD Dresden University of Technology, 01062 Dresden, Germany

[a)] hhchuang@pks.mpg.de
[b)] **Author to whom correspondence should be addressed:** eisfeld@pks.mpg.de

ABSTRACT

We consider assemblies of molecules where the electronic wavefunctions of different molecules do not overlap. Typically, the interaction Hamiltonian between two molecules is then described by their Coulomb interaction, and matrix-elements between products of single-molecule energy eigenstates are calculated using the corresponding (transition) charge densities. In the present work, we compare this approach with one based on (transition) current densities. As an example, we perform calculations for 3,4,9,10-perylenetetracarboxylicacid-dianhydride (PTCDA) molecules in different arrangements. We find that for exact molecular wavefunctions, both methods agree, but there are marked differences for the wavefunctions that we obtained from electronic-structure theory. The main difference can be attributed to the error in the molecular transition energy and results in an arrangement-independent ratio between the interactions calculated with the two approaches. At small separations between the molecules, additional deviations occur, which we trace back to the quality of the molecular electronic wavefunctions. Within both approaches, we calculate interactions for the arrangement of PTCDA on KCl and NaCl surfaces and compare to the ones obtained using the point–dipole approximation. Finally, we provide a simple algorithm that allows fast and accurate calculations of the involved integrals.

I. INTRODUCTION

Many systems in physics, chemistry, biology, or nanotechnology consist of assemblies of particles (atoms, molecules, quantum dots, metal–nanoparticles, etc.) with distances ranging from a few Ångströms to a few nanometers. Examples are pigment protein complexes of photosynthesis,[1–3] molecular aggregates in solution or on surfaces,[4–6] molecules in the vicinity of metal nano-structures,[7,8] or ensembles of (ultra-cold) Rydberg atoms.[9–12] Long-range interactions play an important role in these systems and lead to strong changes in their optical and transport properties. It is, therefore, an important task to evaluate these interactions. It is common to start with eigenstates of the individual molecules. Denoting by $|\phi_a^A\rangle$ the ath eigenstate of particle A, the relevant matrix elements of the long-range interaction $\hat{V}_{\text{int}}$ have the form $\langle\phi_a^A\phi_b^B|\hat{V}_{\text{int}}|\phi_{a'}^A\phi_{b'}^B\rangle$, where $|\phi_{a'}^A\phi_{b'}^B\rangle$ is a product state where particle A is in state a' and particle B is in state b'.[13] For large enough distances between the particles, this interaction can be taken to be the interaction between the *transition point dipoles* of the respective particles. In many situations, however, this approximation is not accurate enough. Then, typically, this interaction matrix element is calculated using the Coulomb interaction between the *transition charge densities* of the two molecules.[2,13,14]

In the present work, we show that one can also calculate the interaction by using the *transition current density* instead of transition charge density. The transition current density also offers the possibility to go beyond the electrostatic approximation and treat molecules at distances that are not small compared to the wavelength of the molecular transition. Despite its fundamental role and widespread use in various disciplines,[15–19] including the theory of molecular assemblies,[20–22] the transition current density, to the best of our knowledge, has never been utilized to calculate intermolecular interactions from *ab initio* wavefunction data. As mentioned above, for not too small distances, the interaction between the molecules

can be well approximated by the interaction of two point dipoles. Common ways to calculate these point dipoles is using the length gauge (which relates to the transition charge density) or the velocity gauge (which relates to the transition current density). It has been realized that when using an exact treatment, the two approaches give the same result. For approximate treatments (e.g., finite basis, non-local potentials, or approximate Hamiltonians), however, they usually differ.[23–27] Clearly, for distances where the point–dipole approximation is applicable, these discrepancies will directly affect the resulting interactions. The questions of interest in this work focus on how the interactions calculated using the two methods (transition charge density and transition current density) behave as a function of distance and relative orientation of the molecules. In addition, we aim to find an efficient and simple way for performing the six-dimensional integral over the densities.

To numerically calculate the interaction matrix elements (either using the transition charge density or the transition current density), we use discretization schemes, i.e., approximating the continuous densities by a finite number of elements. A straightforward discretization scheme is to represent the densities on an equidistant, rectangular grid. Then, at each grid-point, density is represented by the integrated value over the volume associated with that grid point. Let N_A and N_B denote the number of points used to represent the densities of molecules A and B, respectively. Then, the calculation of the interaction matrix element consists of a sum of $N_A \times N_B$ terms. When assessing interactions for numerous molecular arrangements, as in large aggregates with positional disorder,[4,28,29] the number of calculations grows rapidly—and even more so because long-range interactions require calculations not only for nearest neighbors. For the case of the transition charge density, many methods have been developed for that purpose (see, for example, Refs. 2 and 30–32).

Here, we use and investigate a simple and efficient method that can be applied to both the transition charge and the transition current density. This method deterministically clusters points from the initial grid representation, yielding far fewer points than the original N_A and N_B, yet incurring negligible loss of accuracy. As an example, we perform calculations for the molecule 3,4,9,10-perylenetetracarboxylicacid-dianhydride (PTCDA), a well-studied molecule. There are many situations where interaction between different PTCDA are of great importance, e.g., crystals,[33,34] thin films,[35–38] in liquid,[39] helium droplets,[40] various monolayers on metallic, or dielectric surfaces.[41–43] We focus in particular on the arrangements of PTCDA monolayers on NaCl and KCl surfaces.

This paper is organized as follows: In Sec. II, we define the transition charge density and the transition current density, and state their relation to the interaction matrix elements. We discuss briefly the connection to point transition dipoles. In Sec. III, we perform exemplary calculations for PTCDA. We show where our algorithm places point charges and point dipoles and investigate the convergence of the interaction matrix elements (for transitions between the electronic ground and first excited state). We conclude in Sec. IV with a brief summary and an outlook. In Appendix A, we provide details about our algorithm to place the transition charges and the transition dipoles. In Appendix B, we show that a special case of our algorithms gives the so-called extended dipole approximation. In Appendix C, we derive the continuity equation for the transition current, which is then used in Appendix D to show that for exact eigenfunctions the interaction calculated from the transition charge density gives the same value as that calculated using the transition current density.

II. BASIC FORMALISM

A. Description of the individual molecules

Throughout this work, we consider fixed nuclei at position $\boldsymbol{R}_\ell$. We also assume that spin–orbit interaction can be neglected, so that the molecular eigenstates can be written as products of a spatial wavefunction and a spin-function. To keep the notation simple, we consider states with the same spin multiplicity (e.g., singlet states) and do not write the spin part explicitly. The electronic Hamiltonian of individual molecules then reads

$$\hat{H}_{\mathrm{el}} = -\sum_{k=1}^{N_{\mathrm{el}}} \frac{\nabla_k^2}{2} + \sum_{k=1}^{N_{\mathrm{el}}} \sum_{k'>k}^{N_{\mathrm{el}}} \frac{1}{|\boldsymbol{r}_k - \boldsymbol{r}_{k'}|} - \sum_{k=1}^{N_{\mathrm{el}}} \sum_{\ell=1}^{N_{\mathrm{nuc}}} \frac{Z_\ell}{|\boldsymbol{r}_k - \boldsymbol{R}_\ell|}, \tag{1}$$

where $\boldsymbol{r}_k$ label the electronic coordinates and Z_ℓ are the charges of the nuclei. The electronic eigenstates and the corresponding eigenenergies of a single molecule are then determined by

$$\hat{H}_{\mathrm{el}}\, \Psi_a(\boldsymbol{r}_{\{k\}}) = E_a\, \Psi_a(\boldsymbol{r}_{\{k\}}), \tag{2}$$

where $\boldsymbol{r}_{\{j\}}$ is an abbreviation for the set of all electronic coordinates $\boldsymbol{r}_1, \ldots, \boldsymbol{r}_{N_{\mathrm{el}}}$ and a labels the eigenstates. The transition frequencies between the states a and b are defined by

$$\omega_{ab} = E_a - E_b. \tag{3}$$

We use atomic units, unless stated otherwise.

1. Transition charge density

The transition charge density between two molecular eigenstates is[44]

$$\rho_{ab}(\boldsymbol{r}) = \int \mathrm{d}^3 r_{\{k\}}\ \ \Psi_a^*(\boldsymbol{r}_{\{k\}})\hat{\rho}(\boldsymbol{r}, \boldsymbol{r}_{\{k\}})\Psi_b(\boldsymbol{r}_{\{k\}}), \tag{4}$$

with the operator,

$$\hat{\rho}(\boldsymbol{r}, \boldsymbol{r}_{\{k\}}) = \sum_k \delta(\boldsymbol{r} - \boldsymbol{r}_k). \tag{5}$$

Remember that we use atomic units. In SI units in the right-hand side, the delta function is multiplied by the electron charge e. The hat indicates that $\hat{\rho}$ is an operator and not just a scalar function.

Note that the eigenstates are only fixed up to a phase, which implies that the transition densities discussed in the following are also only fixed up to a phase.

2. Electronic transition current and dipole density

The electronic transition current density between the states a and b is defined as[44]

$$\boldsymbol{j}_{ab}(\boldsymbol{r}) = \int \mathrm{d}^3 \boldsymbol{r}_{\{k\}}\ \ \Psi_a^*(\boldsymbol{r}_{\{k\}})\, \hat{\boldsymbol{j}}(\boldsymbol{r}, \boldsymbol{r}_{\{k\}})\, \Psi_b(\boldsymbol{r}_{\{k\}}), \tag{6}$$

with the transition current operator,

$$\hat{\boldsymbol{j}}(\boldsymbol{r}, \boldsymbol{r}_{\{k\}}) = -\frac{\mathrm{i}}{2} \sum_k \left(\delta(\boldsymbol{r} - \boldsymbol{r}_k)\nabla_k - \nabla_k \delta(\boldsymbol{r} - \boldsymbol{r}_k)\right). \tag{7}$$

The integral over the electronic coordinates is evaluated using, e.g., the exponential representation of the delta-function. It is convenient to introduce the *transition dipole density*,[44]

$$\boldsymbol{d}_{ab}(\boldsymbol{r}) = -i\frac{1}{\omega_{ab}}\boldsymbol{j}_{ab}(\boldsymbol{r}) \qquad \text{for} \quad a \neq b, \tag{8}$$

which is proportional to the transition current density. The proportionality factor ω_{ab} appearing in Eq. (8) is just the transition frequency defined in Eq. (3). As for the transition charge density, in general, $\boldsymbol{j}_{ab}$ is complex, but for real wavefunction, it is purely imaginary and thus $\boldsymbol{d}_{ab}$ is real. In the present work, we will deal with real-valued wavefunctions.

B. Interaction between molecules

We now present two ways of calculating the interaction matrix elements between two molecules. One is based on the transition charge density, the other on the transition current density. In Appendix D, we show that the two ways give (for exact electronic eigenfunctions) the same result. We point out that the used formulas do not contain radiation contributions and are only valid for molecular separations that are much smaller than the wavelength of the transition—the case in which we are interested.

1. Using transition charge density

The interaction matrix element between a transition of molecule A and a transition of molecule B is given by (see, e.g., Chap. 9 of Ref. 13)

$$W_{ab,cd}^{(A,B)} = \int \mathrm{d}^3r \int \mathrm{d}^3r' \, \frac{\rho_{ab}^{(A)}(\boldsymbol{r})\, \rho_{cd}^{(B)}(\boldsymbol{r}')}{|\boldsymbol{r}-\boldsymbol{r}'|}, \tag{9}$$

where a and b are the states involved in the transition of molecule A, and c and d are the ones of molecule B. In general, the ρ_{ab} is complex, but for real wavefunction (which we are using in the following), it is real. One should keep in mind that the interaction matrix elements are only determined up to a phase since the underlying wavefunctions are only determined up to a phase.

2. Using electronic transition current and dipole density

The interaction matrix element between a transition of molecule A and a transition of molecule B is given by

$$V_{ab,cd}^{(A,B)} = \int \mathrm{d}^3r \int \mathrm{d}^3r' \left[\boldsymbol{d}_{ab}^{(A)}(\boldsymbol{r})\right]^{\mathsf{T}} \mathbb{T}(\boldsymbol{r},\boldsymbol{r}')\, \boldsymbol{d}_{cd}^{(B)}(\boldsymbol{r}'), \tag{10}$$

with the dipole tensor,

$$\mathbb{T}(\boldsymbol{r},\boldsymbol{r}') = \frac{1}{|\boldsymbol{r}-\boldsymbol{r}'|^3}\left\{\mathbb{1} - 3\frac{(\boldsymbol{r}-\boldsymbol{r}')(\boldsymbol{r}-\boldsymbol{r}')^{\mathsf{T}}}{|\boldsymbol{r}-\boldsymbol{r}'|^2}\right\}. \tag{11}$$

This tensor fulfills $\mathbb{T}(\boldsymbol{r},\boldsymbol{r}') = \mathbb{T}(\boldsymbol{r}-\boldsymbol{r}')$ and describes the interaction between dipoles located at $\boldsymbol{r}$ and $\boldsymbol{r}'$, respectively. For exact transition charge densities, ρ_{ab}, and exact dipole densities, $\boldsymbol{d}_{ab}$, the interaction matrix elements V and W, as given in Eqs. (9) and (10), do agree (see Appendix D). Note, in particular, that no multipole expansion has been made to arrive at (10). In Sec. II D the point–dipole approximation is briefly discussed.

We should note that Eqs. (9) and (10) with (11) are only valid for static Coulomb interactions and the longitudinal part of the dyadic Green-function,[45] respectively. Those approximations are useful for intermolecular distances smaller than the wavelength of the transition. In order to treat molecules at larger distances, where transversal (i.e., radiation) components might become relevant, one has to replace $\mathbb{T}$ in Eq. (10) by the full Green-function.

C. Numerically calculating the integral appearing in the interaction

We aim at evaluating the integrals appearing in Eqs. (9) and (10) as sums of a finite number of transition charges/dipoles located at appropriate positions, i.e.,

$$W \approx \sum_{n=1}^{N_A}\sum_{m=1}^{N_B} \frac{q_n^A q_m^B}{|\boldsymbol{r}_n^A - \boldsymbol{r}_m^B|}, \tag{12}$$

$$V \approx \sum_{n=1}^{N_A}\sum_{m=1}^{N_B} \left(\boldsymbol{d}_n^A\right)^{\mathsf{T}} \mathbb{T}(\boldsymbol{r}_n^A, \boldsymbol{r}_m^B)\, \boldsymbol{d}_m^B, \tag{13}$$

where $\boldsymbol{r}_n^{A/B}$ are the positions at which $N_{A/B}$ charges $q_n^{A/B}$ or dipoles $\boldsymbol{d}_n^{A/B}$ are located. For readability, we do not explicitly keep the labels of the two states involved in the transition. The n-summation runs over molecule A and the m-summation over molecule B. Equation (12) is the Coulomb interaction between charges at different particles, and Eq. (13) represents the interaction between a distribution of dipoles at molecule A with a distribution of dipoles of molecules B. The summation of Eqs. (12) and (13) contain $N_{\mathrm{sum}} = N_A \times N_B$ terms.

The summations in Eqs. (12) and (13) represent a very general description. If one uses a dense regular grid for $\boldsymbol{r}_n^{A/B}$, with $q_n^{A/B}$ or $\boldsymbol{d}_n^{A/B}$ obtained with an electronic-structure calculations, they are essentially exact. Therefore, we will use those values later on as reference values. The drawback is the high computational cost. For example, when one takes the positions $\boldsymbol{r}_n$ on a regular grid with 100 points in each spatial direction, one would have to sum up $10^{6\times2}$ terms. The other extreme is considering the molecules as point dipoles, as discussed in the following. In this case, we have $N_A = N_B = 1$ in Eq. (13). The prize one has to pay is an approximate description, particularly for small inter-molecular distance. Here, we aim at intermediate numbers $N_{A/B}$, say a few hundred, which makes the computation (even for many pairs of molecules) tractable without compromising much on the final accuracy. We give a detailed description of the fast and simple algorithm that we propose in Appendix A.

Note that when one is dealing with identical molecules, it is convenient to perform this calculation only for one molecule and then shift and rotate the molecular frame into the arrangement of the interacting molecules.

D. Connection to transition point dipoles

It is well known how various types of point dipoles are related to the transition charge density and to the transition current density.

1. Point dipole from the transition charge density

A multipole expansion leads to the *transition point dipole,*

$$\boldsymbol{\mu}_{ab} = \int \mathrm{d}^3r\, \boldsymbol{r}\, \rho(\boldsymbol{r}), \tag{14}$$

located at position $\boldsymbol{R}_{ab} = (\int \mathrm{d}^3 r\, \boldsymbol{r}|\rho(\boldsymbol{r})|)/(\int \mathrm{d}^3 r\, |\rho(\boldsymbol{r})|)$. This expression is often referred to as the transition point dipole in *length gauge*.[44] In Appendix B, we also provide the often used *extended dipole*.[32]

2. Point dipole from the transition current density

From Eq. (6), one directly obtains a point transition dipole,

$$\boldsymbol{d}_{ab} = -\mathrm{i}\frac{1}{\omega_{ab}} \int \mathrm{d}^3 \boldsymbol{r}\, \boldsymbol{j}_{ab}(\boldsymbol{r}), \tag{15}$$

which is located at $\int \mathrm{d}^3 r\, \boldsymbol{r}\, |\boldsymbol{j}_{ab}(\boldsymbol{r})| / \int \mathrm{d}^3 r |\boldsymbol{j}_{ab}(\boldsymbol{r})|$. This is denoted as *transition dipole from the velocity gauge* in Ref. 44.

3. Interactions

Within the point–dipole approximation, the interactions of Eqs. (12) and (13) become

$$W_{\mathrm{point}} \approx \left(\boldsymbol{\mu}^A\right)^{\mathsf{T}} \mathbb{T}(\boldsymbol{R}^A, \boldsymbol{R}^B)\, \boldsymbol{\mu}^B, \tag{16}$$

$$V_{\mathrm{point}} \approx \left(\boldsymbol{d}^A\right)^{\mathsf{T}} \mathbb{T}(\boldsymbol{R}^A, \boldsymbol{R}^B)\, \boldsymbol{d}^B, \tag{17}$$

where we have not explicitly written the labels of the participating states. For exact eigenfunctions and eigenenergies, the point dipole in length gauge is equal to the dipole from velocity gauge, and therefore, both interaction matrix elements will be the same.

III. EXEMPLARY CALCULATIONS FOR PTCDA

In the following, we will consider the interaction of a pair of two identical molecules. We have chosen PTCDA, a flat molecule with 38 atoms; see Fig. 1, where we show the structure in the bottom panels. We consider neutral and closed-shell PTCDA molecules. We are interested in transitions between the electronic ground state (g) and the first excited state (e). For the results shown in the following, these states are obtained from electronic-structure calculations using Psi4,[46] release 1.8. The level of theory used to calculate the molecular wavefunctions of the ground and first excited states is configuration interaction singles (CIS)[47,48] with a restricted active space (2e,2o) consisting of LUMO and HOMO. We used the spherical harmonic atomic orbital basis set 6-311G(2d,2p).[49] We did not impose the D_{2h} symmetry. From these states, the densities are computed and represented on a regular grid using ORBKIT version 1.1.0.[17] The resolution of the grid is $\Delta x = \Delta y = \Delta z = 0.0529$ Å. We have taken the grid sufficiently large to ensure it contains the complete densities. The number of grid points for the three directions are $N_x = 281$, $N_y = 201$, and $N_z = 101$, respectively. Correspondingly, the covered volume is $14.8 \times 10.6 \times 5.3$ Å^3. The transition dipole density $\boldsymbol{d}_{\mathrm{eg}}(\boldsymbol{r})$ is obtained from Eq. (8) using the transition frequency ω_{eg} as obtained from Psi4.

A. Point dipoles

From ORBKIT, we also obtain the point dipoles (14) and (15), which in Ref. 44 are denoted as "dipole in length gauge" and "dipole *from* velocity gauge," respectively. We find that both point in the same direction (along the x axis) but have different magnitudes: $|\boldsymbol{\mu}_{\mathrm{eg}}| = 10.60$ D and $|\boldsymbol{d}_{\mathrm{eg}}| = 7.84$ D, respectively. For a fully converged electronic-structure theory calculation, these values should agree. A difference between them gives hints on the quality of the obtained energies and wavefunctions.[44] While in Eq. (14) only the wavefunctions appear, in Eq. (15), the transition frequencies also enter. From our quantum chemistry calculations, we have $\omega_{\mathrm{eg}} \approx 29\,547\ \mathrm{cm}^{-1}$. Absorption and fluorescence experiments of PTCDA in He nanodroplets (which are close to vacuum conditions at zero temperature), however, show the value $\omega_{\mathrm{eg}}^{\mathrm{exp}} \approx 21\,000\ \mathrm{cm}^{-1}$.[50] This gives a ratio $\omega_{\mathrm{eg}}^{\mathrm{exp}}/\omega_{\mathrm{eg}} \approx 0.71$. This is close to the ratio $s = |\boldsymbol{d}_{\mathrm{eg}}|/|\boldsymbol{\mu}_{\mathrm{eg}}| \approx 0.74$ between the dipole from velocity gauge and the dipole in length gauge. This suggests that the main difference between $\boldsymbol{d}_{\mathrm{eg}}$ and $\boldsymbol{\mu}_{\mathrm{eg}}$ is due to the bad quality of the quantum–chemical transition energy. More accurate calculations quickly become much more expensive and do not change our general observations discussed in the following. Note that in the definition of the transition density Eq. (8), the same factor ω_{eg} appears and, therefore, it appears squared

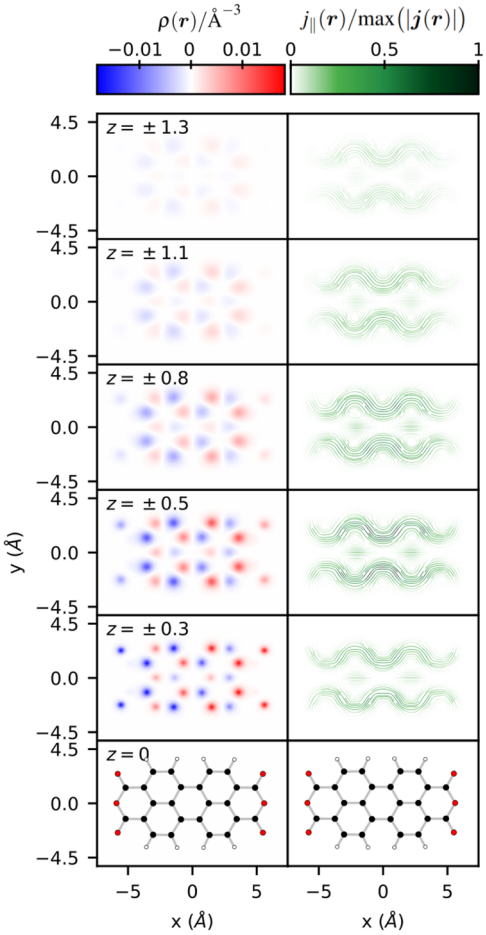

FIG. 1. Structure of PTCDA and its transition densities. The structure is shown in the bottom panels. The planar PTCDA molecule is taken to lie in the x–y plane ($z = 0$). The different panels show cuts through the transition charge density (left column) and the transition dipole density (right column) parallel to the x–y plane at various values of z (indicated in the panels). Note that for $z = 0$, the densities are zero.

in the interaction Eq. (10). We come back to this point later in this article.

B. The transition densities

The transition current density and the transition charge density as obtained from ORBKIT are shown in Fig. 1. For better representation, we show stream-line plots (obtained using matplotlib) for the transition current density. We present the density distributions for cross sections parallel to the xy-plane at the z-values indicated in each panel. Note the symmetry with respect to the molecular plane ($z = 0$). For the transition current density, the vector field has only very small components in the z-direction.

These representations on a dense grid will now be replaced by a smaller number of point charges or point dipoles. In Fig. 2, we show examples of the placement of the point charges q_n and point dipoles $\boldsymbol{d}_n$. These q_n and point dipoles $\boldsymbol{d}_n$ with their respective positions $\boldsymbol{r}_n$ then enter Eqs. (12) and (13). The absolute values $|q_n|$ and $\|\boldsymbol{d}_n\|$ are represented by the radii of the spheres and the lengths of the arrows, respectively. We show results for different total numbers of transition charges/dipoles obtained using the algorithm described in Appendix A. For the charge density, we have used the variant described at the end of Appendix A.

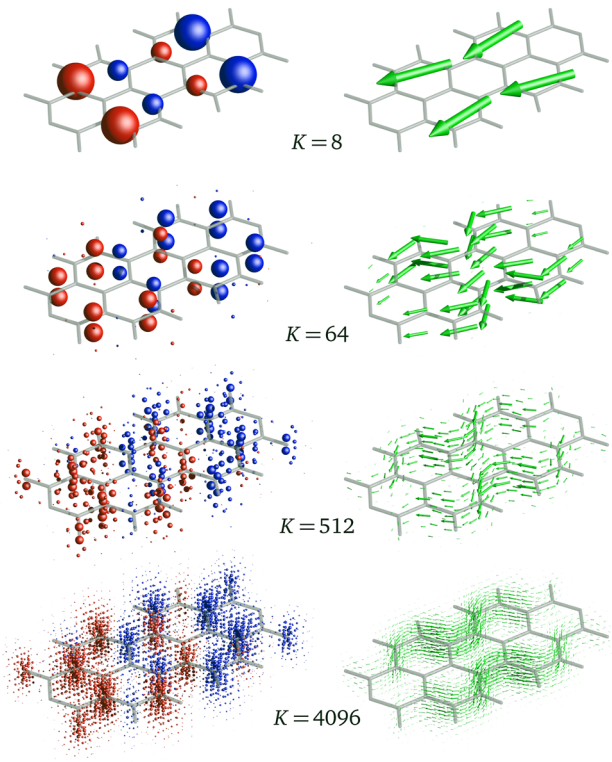

FIG. 2. Approximating the continuous transition charge density (left column) and dipole density (right column) by a finite number K (specified in each row) of charges or dipole vectors. The radii of the spheres (lengths of the arrows) are proportional to the values of the charge $|q_m|$, with the color indicating the sign (dipole strength $\|\boldsymbol{d}_m\|$). Note that the spheres or arrows can be too small to be visible and thus the numbers of charges and dipoles may seem to be different, although they are not.

C. The interaction between molecules

We come now to the main part of the present work, where we investigate the interaction obtained from the transition charge density and the transition current density. In addition to the question if the two quantities give the same value of the interaction, we are also interested in the convergence with the number of charges/dipoles. We exemplify our findings for a few selected molecular arrangements, as shown in the upper row of Fig. 3. With R, we denote the magnitude of the center-to-center distance between the two PTCDA molecules. For all calculations, the (grid-)representation of PTCDA, discussed at the beginning of this section, has been used. For molecules that are shifted and rotated with respect to the molecule considered above, we simply apply the same shift and rotation to the points (and dipole-vectors) obtained for the original position and orientation.

In the second row [Fig. 3(a)], we show the distance dependence of the interaction. To facilitate the comparison between W and V from Eqs. (9) and (10), respectively, we have multiplied V by a factor $s^2 = \|\boldsymbol{\mu}_{\mathrm{eg}}\|^2/\|\boldsymbol{d}_{\mathrm{eg}}\|^2 \approx 1.81$, where $\boldsymbol{\mu}_{\mathrm{eg}}$ and $\boldsymbol{d}_{\mathrm{eg}}$ are the point dipoles from Eqs. (14) and (15) above. Note that for this comparison, we could have distributed this factor s^2 in an arbitrary way among W and V. However, the discussion of Subsection III A suggests the present choice.

In each panel of Fig. 3(a), we show four curves: the results obtained from the dipole approximation W_{point} and V_{point} (both indicated by the black dotted lines), which are exactly identical because of our scaling of V with s^2. The other two curves are interactions obtained from the densities on the fine grid discussed above (0.1 bohr resolution). We denote the respective interactions by V_{grid} (blue-solid) and W_{grid} (red-dashed). For an even finer grid, there would be very small changes (not visible on the present scale and typically not relevant for practical purposes, where a relative error of ~1% is more than sufficient).

One clearly sees that the grid calculations differ at small distances significantly from the point–dipole interactions V_{point} and W_{point}. For all cases shown, one sees that for distances $R \gtrsim 2.5$ nm, the point–dipole approximation agrees well with the results of the grid-based calculations. However, for smaller distances, marked differences become visible. As expected, these deviations grow for decreasing distances. More interesting for us is the difference between W_{grid} and V_{grid}. We see that, both on the logarithmic and the linear scales, these curves are nearly indistinguishable. This is an encouraging result. We want to stress that this agreement is not guaranteed and seems to require sufficiently accurate wavefunctions from the electronic structure calculations. If the wavefunctions would be highly accurate, then the difference between W and V would be mainly caused by the error in the transition frequency ω_{eg} (and only slightly by the error in the wavefunction). Then, we would find that for a fine enough grid, the interaction calculated from both methods would agree for all molecular arrangements (because we have taken the error of ω_{eg} into account via the scaling by s^2). Since there is agreement for large distances, our results show that no global (i.e., R-independent) scaling is possible. We have found that for smaller basis sets, the difference between W_{grid} and V_{grid} can be quite large (e.g., for the 3-21G basis set, we found relative differences about 7% for the arrangement of the second column of Fig. 3).

In the two bottom rows [Figs. 3(b) and 3(c)], we show the convergence of the interaction with respect to the number K of

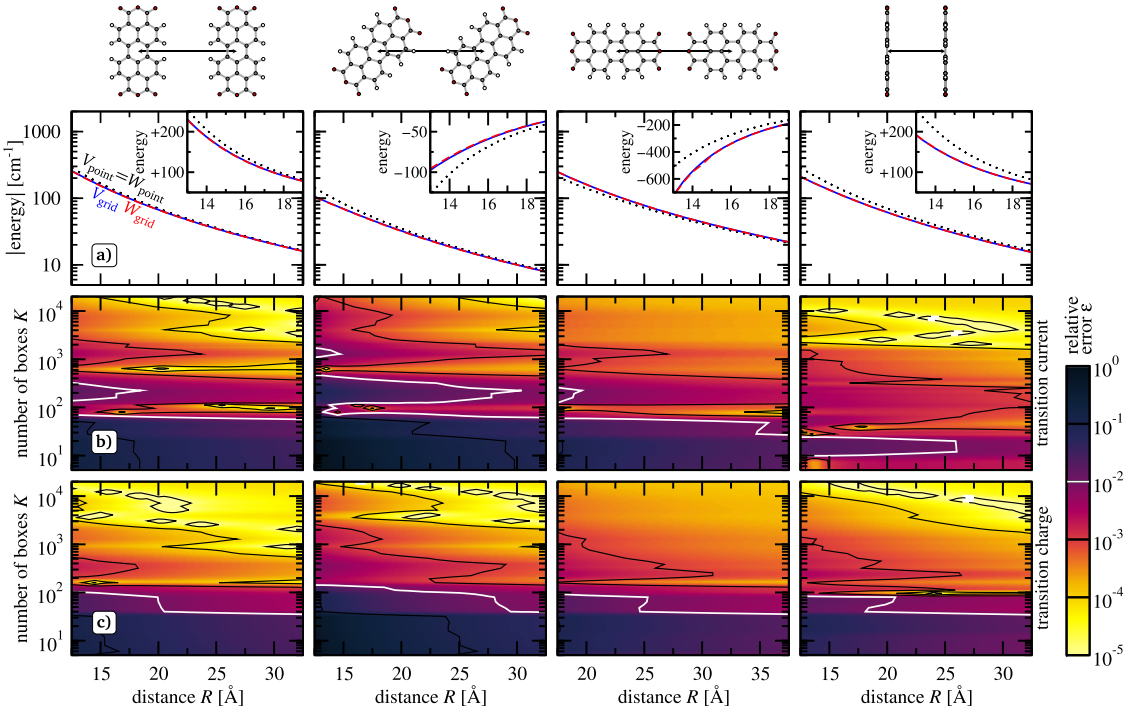

FIG. 3. Distance dependence and convergence of the interaction for selected molecular arrangements (shown in the top row). Row (a): interaction calculated using the full original grid using Eq. (13), blue lines, and (12), the red dashed lines, together with the point dipole results Eqs. (16) and (17) (black dotted curves). Note that we have scaled the results that come from the current by the factor S given in the main text. That enforces that the point dipole curves lie exactly on top of each other. One also sees that the curves of the full calculation are indistinguishable. To be better able to compare the curves over a large range of distances, we use a logarithmic energy scale and plot the absolute value of the interaction. The insets show the important case of small distances where we kept the sign of the interactions, which depends on the dimer geometry. Row (b): convergence with respect to the number of dipoles used in Eq. (13). Note the logarithmic color bar. Row (c): same as third row, but now for the number of point charges used in Eq. (12). The center-to-center distance is denoted by R. Note the different ranges of the distance R for the four cases. The contour line with a relative error of $\varepsilon = 1\%$ is plotted in white.

charges/dipoles used to approximate the density. The bottom row [Fig. 3(c)] is for the transition charge density and row above [Fig. 3(b)] for the transition current density. As reference, we have chosen the values W_{grid} and V_{grid} obtained from the fine grid [i.e., the values of row (a)]. We show the relative errors $\varepsilon_K(R) = |E_K(R) - E_{\text{grid}}(R)|/|E_{\text{grid}}(R)|$, where $E_K(R)$ denotes the interaction energy (either W or V, respectively) obtained using K charges/dipoles and $E_{\text{grid}}(R)$ is the respective reference calculation [$W_{\text{grid}}(R)$ or $V_{\text{grid}}(R)$, respectively]. Note the logarithmic scale of the color-bar. We see that upon increasing the number K of charge/dipoles by an order of magnitude, the relative error decreases roughly by an order of magnitude. This is a very rough estimation since the convergence is typically not uniformly. There is only a weak dependence on the relative error on the distance R between the molecules, with a slightly faster convergence for larger distances. In general, the convergence of the transition charges is slightly faster than that of the transition current calculations. One needs roughly five times more dipoles than charges to have the same accuracy. However, both often show a quite non-monotonic behavior and general statements are difficult to make. As mentioned above, for practical purposes, typically a relative error of 1% is more than sufficient. That means that for around 1000 points, we have this accuracy for the investigated distances and orientations.

1. Values for PTCDA in special arrangements relevant for monolayers on dielectric surfaces

Here, we provide values calculated for specific arrangements that PTCDA molecules form on dielectric ionic surfaces. In particular, we look at arrangements on KCl and on NaCl. In both cases, the PTCDA molecules form regular two-dimensional pattern. On KCl, a so-called brick-wall pattern is found,[51] where all molecules lie flat on the surface and their long axes are parallel. On NaCl, the orientations of the long axes alternate by 90°.[42] To understand the optical and transport properties of these systems, it is crucial to know the interactions.[43] In Fig. 4, we show values for the most important interactions between pairs of molecules. As expected from the results of Fig. 3, for the small distances, one has quite large differences between the point–dipole approximation and the more refined treatment using the dipole density.

Finally, we would like to point out that our calculations are for molecules in free space, ignoring effects of the surface. In addition to small modifications of the PTCDA structure (which also slightly modify the transition densities), the presence of the surface also changes the form of the interaction between the molecules. A simple way how to approximately take this modification into account is via image transition charges/dipoles.

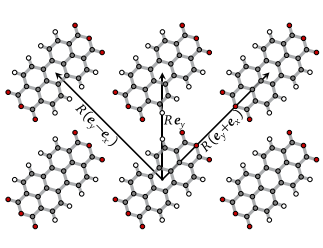

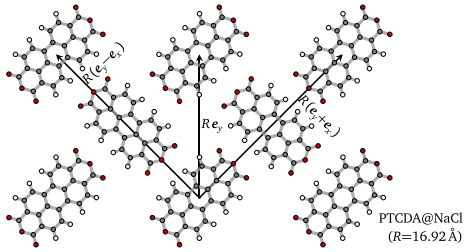

center-to-center vector		Re_y	$R(e_y+e_x)$	$R(e_y-e_x)$
density (on grid)	W_{grid}	−103.7	−231.6	+92.9
	V_{grid}	−56.0	−128.2	+51.2
	$s^2 V_{\text{grid}}$	−101.4	−232.1	+92.6
point dipoles	W_{point}	−138.6	−196.1	+98.0
	V_{point}	−76.6	−108.3	+54.1
	$s^2 V_{\text{point}}$	−138.6	−196.1	+98.0

center-to-center vector		Re_y	$R(e_y+e_x)$	$R(e_y-e_x)$
density (on grid)	W_{grid}	−51.0	−89.5	+39.7
	V_{grid}	−27.9	−49.5	+21.9
	$s^2 V_{\text{grid}}$	−50.5	−89.5	+39.6
point dipoles	W_{point}	−57.8	−81.7	+40.9
	V_{point}	−31.9	−45.1	+22.6
	$s^2 V_{\text{point}}$	−57.8	−81.7	+40.9

FIG. 4. Interaction energies of pairs of PTCDA molecules in the arrangement on KCl[52] (left) and on NaCl[42] (right). Top panel: sketch of the respective arrangements. Bottom panel: interaction energies of (9) and (10) in units of cm^{-1} for three different dimer structures given by the center-to-center vector connecting both molecules in the dimer, as shown in the sketches above, which also give the length scales R. Values from both transition charge and transition current density (provided by ORBKIT on a grid with a spacing of 0.1 bohr for all axis) as well for the corresponding point dipoles are given. Hereby, we use the scaling factor s^2 discussed in the text, cf. Sec. III C, to correct the values for V.

IV. CONCLUSIONS

In this work, we have investigated the possibility to use the transition current density of molecules to calculate the long-range interaction matrix elements between pairs of molecules. In particular, we have focused on transitions between the ground and the first excited electronic state. The corresponding matrix elements are relevant for the transfer of excitation from one molecule to another. The formalism can of course directly be applied to transitions between other states. In addition, the two molecules can have different transitions. We have focused on distances between the molecules that are much shorter than the wavelength corresponding to the molecular transitions. This is the typical situation of molecular aggregates, where the relevant distances between molecules are in the order of a few nanometers, whereas the wavelength is several hundred nanometers. In our calculations, we used the molecule PTCDA as an example.

We found that the results obtained from the transition charge density and the transition current density deviate quite significantly from each other. The results obtained from the transition charge density are roughly a factor of two larger than the ones obtained from the transition current density. For exact eigenstates and eigenenergies of the molecular electronic Hamiltonian, the results from both approaches would agree. For approximate eigenenergies and eigenfunctions, this needs no longer be the case. Note that the eigenenergies enter via Eq. (8) into our calculation of the dipole density. However, this is simply a scaling factor, common to all arrangements of the monomers. Thus, changes of the relative difference between the two methods when changing the arrangement reflects the accuracy of the wavefunction. We found that there are deviations only at very close distances.

In the calculations shown, we used the 6-311G(2d,2p) basis set and found a difference smaller than 1%. If the basis set cannot describe the relevant parts of the densities accurately enough, then these deviations become larger. For example, for the 3-21G basis set, we found relative differences up to ~7%. For the algorithm used in the present work, the size and resolution of the grid on which the densities are evaluated is also important for the accuracy of the results. In principle, one could calculate the interaction directly from the wavefunction obtained from electronic structure theory by performing a sum of Coulomb integral over products of primitive Gaussians (transition charge density) or "dipole integrals" over primitive Gaussians. We used here a simple, efficient, but nevertheless accurate algorithm, where the transition densities of a molecule are approximated by a finite number of point charges (charge density) or point dipoles (current density). We used a simple algorithm to construct these charges/dipoles, which aims at reproducing the continuous densities as good as possible. We found that even at very short distances between the molecules, only on the order of 1000 charges/dipoles are needed per molecule to calculate the interaction between the molecules sufficiently accurately. The number of charges/dipoles could further be reduced by taking into account the strong distance dependence of the interaction. This can be done, for example, by increasing point density in regions of a molecule that are in closer proximity to the other molecule. This can be easily done, by not making the divisions of the boxes symmetrically, but preferring parts that are closer to the other molecule. This can be done either by placing the division planes of the boxes asymmetrically or to give larger weight in selecting a box closer to the other molecule. Nevertheless, the number of points needed in our present approach is small enough to allow efficient and accurate calculations and after obtaining the charges/dipoles for one molecule, it can be directly applied to an assembly of many identical molecules.

We would like to note that the representation by a finite number of point charges/dipoles can also be used to estimate the changes compared to the point–dipole approximation, similar to

what has been done before.[32,53] In that way, one can, for example, for PTCDA@KCl (see Fig. 4, left panel) easily rationalize why the interaction for the $(\boldsymbol{e}_x + \boldsymbol{e}_y)$ direction becomes more negative compared to the point–dipole approximation, while it becomes less negative for the $\boldsymbol{e}_y$ direction.

Since the interaction matrix elements calculated from the transition charge density is quite different from the one calculated using the current density, it is an important question which of the two values are closer to the correct result. Although we cannot make a definite statement, we have some indications in favor of the transition charge density: As discussed in Sec. III A, in the formula of the dipole density, the transition frequency explicitly enters. The transition frequencies that we have obtained from our electronic structure calculations deviate from the experimental value by more than 30%. If one uses the experimental value of the transition frequency, then the two interaction energies are very close to each other for all investigated arrangements. This suggests that, when using the transition current density, one should use the experimental transition frequency when calculating the transition dipole density. As an alternative to using the experimental transition frequency, one can also scale the transition dipole density such that the point dipole from velocity gauge (15) is equal to the one in length gauge (14), as done in the present work. Following this strategy, in principle, both densities can then be used to calculate the interaction. It should be kept in mind, that the formulas Eqs. (9) and (10) with Eq. (11) are only valid for distances between the molecules that are much smaller than the wavelength of the transition. In order to treat larger distances, one can in the transition current interaction replace $\mathbb{T}$ in Eq. (10) by the full Green tensor,

$$\mathbb{G}(\boldsymbol{r},\boldsymbol{r}';\omega) = \left(\mathbb{I} - \frac{1}{k^2}\nabla\otimes\nabla'\right)\frac{\mathrm{e}^{\mathrm{i}k|\boldsymbol{r}-\boldsymbol{r}'|}}{|\boldsymbol{r}-\boldsymbol{r}'|} \quad \text{with } k = \frac{\omega}{c}. \tag{18}$$

In addition, for small distances, there are instances, in which the transition current density might be preferable. For example, when the molecules are in the vicinity of other (macroscopic) bodies, it might be more convenient to use the transition current. In that case, the interaction will be modified. This situation can be treated using macroscopic quantum electrodynamics.[18,22] This would lead to an evolution equation for the systems density matrix where the interaction matrix elements would have a modified real part complemented by an imaginary part, which becomes particularly important for metallic objects. In addition to the modifications of the interaction elements described above, the surface also directly influences the electronic wavefunctions of the individual molecules. For example, an ionic surface (such as KCl or NaCl) creates an electric field in which the molecules are placed. This can lead to shifts of the eigenenergies and also change the electronic wavefunctions. Even the structure of the molecule can be affected. A practicable way to include such effects into the present framework is to perform the electronic structure theory using the structure of the molecule on the surface and adding an appropriate external field. In any case, we believe that the results presented in the present paper will be helpful in developing an appropriate treatment of molecular assemblies on surfaces.

ACKNOWLEDGMENTS

G. H.-H. Chuang acknowledges support from the Max-Planck Gesellschaft via the MPI-PKS visitors program. A.E. acknowledges support from the DFG via a Heisenberg fellowship (Grant No. EI 872/10-1).

AUTHOR DECLARATIONS

Conflict of Interest

The authors have no conflicts to disclose.

Author Contributions

Grace Hsiao-Han Chuang: Formal analysis (supporting); Methodology (supporting); Visualization (equal); Writing – original draft (supporting); Writing – review & editing (equal). **Ulf Saalmann**: Formal analysis (equal); Validation (equal); Visualization (lead); Writing – review & editing (equal). **Alexander Eisfeld**: Conceptualization (lead); Formal analysis (equal); Methodology (equal); Validation (equal); Visualization (supporting); Writing – original draft (lead); Writing – review & editing (equal).

DATA AVAILABILITY

The data that support the findings of this study are available from the corresponding author upon reasonable request.

APPENDIX A: ALGORITHM TO REDUCE THE NUMBER OF POINT TRANSITION CHARGES/DIPOLES

The presented algorithm has been inspired by so-called hierarchical tree codes.[54] Those were originally developed for gravitational problems, but later also applied to Coulomb systems.[55]

1. Basic iteration procedure

The basic algorithm works on a *positive-valued* density $p(\boldsymbol{r})$. Based on this density, the space is iteratively divided into K rectangular volumes (boxes). Initially, we take a box that includes the complete molecule.

Each iteration step starts with a set of k $(< K)$ boxes. For each box, we calculate the volume $V_j = \int_j \mathrm{d}^3 r$ and the integrated density $Q_j = \int_j \mathrm{d}^3 r p(\boldsymbol{r})$, with $\int_j$ denoting an integral over box j. From this set of boxes $(j = 1, \ldots, k)$, we select the one with the largest volume-weighted integrated density $\max_j\{Q_j V_j\}$. One might consider other "weights" for this selection, but the one mentioned turned out to be the most efficient one. Now, we divide this box at the middle of its longest side, resulting in two boxes with the same shape, which replace the selected box. Thus, the number of boxes has increased by one, $k \to k + 1$. This step is repeated until $k = K$.

2. Application to general densities

Neither the transition charge density nor the transition current density is a positive density, as required in the above-mentioned algorithm. The transition charge density is a scalar function, but it typically contains positive and negative values (in general, it is even a complex function). The transition current density is a vector field. Therefore, in a first step, we take the absolute value either $p(\boldsymbol{r}) = |\rho(\boldsymbol{r})|$ or $p(\boldsymbol{r}) = \|\boldsymbol{d}(\boldsymbol{r})\|$ to obtain a positive density. The algorithm from above can then be directly applied to the so obtained functions.

After the complete set of boxes has been created, for each box j, the charge q_j or the dipole $\boldsymbol{d}_j$ and its corresponding position is calculated. To this end, we calculate the "center-of-mass" position $\boldsymbol{r}_j = \int_j \mathrm{d}^3r\, \boldsymbol{r}|\rho(\boldsymbol{r})| / \int_j \mathrm{d}^3r\, |\rho(\boldsymbol{r})|$ or $\boldsymbol{r}_j = \int_j \mathrm{d}^3r\, \boldsymbol{r}\|\boldsymbol{d}(\boldsymbol{r})\| / \int_j \mathrm{d}^3r\, \|\boldsymbol{d}(\boldsymbol{r})\|$. At that position $\boldsymbol{r}_j$, we place the charge $q_i = \int_j \mathrm{d}^3r\rho(\boldsymbol{r})$ or the dipole $\boldsymbol{d}_j = \int_j \mathrm{d}^3r\boldsymbol{d}(\boldsymbol{r})$, respectively.

It is advantageous to remove boxes with densities that are very small within the box. This is in particular necessary, when one has chosen initially a rather large box. The problem that can arise when calculating the interaction is that two points of different particles are very close and although the corresponding charge/dipole is very small, the inverse power of the distance dependence creates a huge interaction (to get accurate results would require high numerical precision).

For the transition dipole density, we used the algorithm as described above. However, for the transition charge density, we used a slightly improved variant, which is described in the Appendix A 3.

3. Alternative way to treat real valued transition charge densities

For a real-valued transition charge density, one can first decompose the density in a positive-valued part and into a negative-valued part. For both parts, one can apply the algorithm from above separately. Note that now the total number of points is $K = K_{\mathrm{pos}} + K_{\mathrm{neg}}$, where K_{pos} and K_{neg} denote the number of boxes used for the positive and negative part of the transition charge density. For the calculations presented in this manuscript, we used this method (with $K_{\mathrm{pos}} + K_{\mathrm{neg}}$). This is the algorithm that we used in the present paper.

If one simply takes one box for the positive and negative part, then this corresponds to the extended-dipole approximation,[32] which we briefly discuss next.

APPENDIX B: THE EXTENDED TRANSITION DIPOLE

From Eq. (4), one can obtain an extended dipole by treating the positive and negative parts of $\rho_{ab}(\boldsymbol{r})$ separately. We define

$$\rho^{\pm}_{ab}(\boldsymbol{r}) = \begin{cases} \rho_{ab}(\boldsymbol{r}) : \rho_{ab}(\boldsymbol{r}) \gtrless 0, \\ 0 : \text{otherwise.} \end{cases} \tag{B1}$$

The "extended dipole" is then given by the charges,

$$Q^{\pm}_{ab} = \int \mathrm{d}^3r\, \rho^{\pm}_{ab}(\boldsymbol{r}), \tag{B2}$$

located at positions,

$$\boldsymbol{R}^{\pm}_{ab} = \int \mathrm{d}^3r\, \boldsymbol{r}|\rho^{\pm}_{ab}(\boldsymbol{r})| / Q^{\pm}_{ab}. \tag{B3}$$

This is a special case of the method discussed at the end of Appendix A.

For neutral molecules, with $Q^{+}_{ab} = -Q^{-}_{ab}$, one can obtain the *point–dipole* as $\boldsymbol{\mu}_{ab} = Q^{+}_{ab}\boldsymbol{R}^{+}_{ab} + Q^{-}_{ab}\boldsymbol{R}^{-}_{ab} = \int \mathrm{d}^3r\, \boldsymbol{r}\rho(\boldsymbol{r})$ located at position $\boldsymbol{R}_{ab} = (\boldsymbol{R}^{+}_{ab} + \boldsymbol{R}^{-}_{ab})/2$, in accordance with the formulas of the main text.

APPENDIX C: THE "CONTINUITY EQUATION" FOR THE TRANSITION CURRENT

In this appendix, we derive the "continuity equation,"

$$\nabla \cdot \mathbf{j}_{ba}(\mathbf{r}) = \mathrm{i}(E_a - E_b)\rho_{ba}(\mathbf{r}) \tag{C1}$$

directly using basic properties of the Hamiltonian and the definitions of the transition charge and current densities, without the need to introduce a time dependence or use a classical analogy. To do so, we start with the identity,

$$\Psi^*_b \hat{H}\Psi_a - \Psi_a(\hat{H}\Psi_b)^* = (E_a - E_b)\Psi^*_b\Psi_a. \tag{C2}$$

The two terms on the left-hand side can be written as

$$\Psi^*_b \hat{H}\Psi_a = -\frac{1}{2}\sum_{i=1}^{N_e} \Psi^*_b \nabla^2_i \Psi_a + (\text{potential terms}), \tag{C3a}$$

$$\Psi_a(\hat{H}\Psi_b)^* = -\frac{1}{2}\sum_{i=1}^{N_e} (\nabla^2_i \Psi_b)^* \Psi_a + (\text{potential terms}). \tag{C3b}$$

Since all potential energy terms (including electron–electron repulsion) are real and symmetric in the particle coordinates, their contributions cancel in the subtraction above. We, therefore, obtain

$$(E_a - E_b)\Psi^*_b\Psi_a = -\frac{1}{2}\sum_{i=1}^{N_e} \left(\Psi^*_b \nabla^2_i \Psi_a - (\nabla^2_i \Psi^*_b)\Psi_a\right). \tag{C4}$$

We now multiply both sides of Eq. (C4) by $\sum_{i=1}^{N_e} \delta(\mathbf{r} - \mathbf{r}_i)$ and integrate over all coordinates to obtain

$$\int \mathrm{d}^{3N}r \sum_{i=1}^{N_e} \delta(\mathbf{r} - \mathbf{r}_i)(E_a - E_b)\Psi^*_b\Psi_a = -\frac{1}{2}\sum_{i=1}^{N_e} \int \mathrm{d}^{3N}r\, \delta(\mathbf{r} - \mathbf{r}_i)\left(\Psi^*_b \nabla^2_i \Psi_a - (\nabla^2_i \Psi^*_b)\Psi_a\right). \tag{C5}$$

The left-hand side is $(E_a - E_b)\rho_{ab}(\boldsymbol{r})$. Using the identity,

$$\Psi^*_b \nabla^2_i \Psi_a - (\nabla^2_i \Psi^*_b)\Psi_a = \nabla_i \cdot \left(\Psi^*_b \nabla_i \Psi_a - (\nabla_i \Psi^*_b)\Psi_a\right), \tag{C6}$$

the right-hand side of (C5) becomes

$$-\nabla \cdot \left(\frac{1}{2}\sum_{i=1}^{N_e} \int \mathrm{d}^{3N}r\, \delta(\mathbf{r} - \mathbf{r}_i)\left(\Psi^*_b \nabla_i \Psi_a - (\nabla_i \Psi^*_b)\Psi_a\right)\right), \tag{C7}$$

which is, by means of Eqs. (6) and (7), equal to $\mathrm{i}\nabla \cdot \boldsymbol{j}_{ba}$.

We note that the continuity equation can also be derived using the Heisenberg equation of motion for the charge density operator.

APPENDIX D: EQUIVALENCE OF THE INTERACTION MATRIX ELEMENTS *V* AND *W*

In this appendix, we show the equivalence of Eqs. (9) and (10), i.e., we show $W^{(A,B)}_{ab,cd} = V^{(A,B)}_{ab,cd}$. We start with Eq. (10). Using $\mathbb{T}(\boldsymbol{r}, \boldsymbol{r}') = \nabla_{\boldsymbol{r}} \otimes \nabla_{\boldsymbol{r}'} \frac{1}{|\boldsymbol{r} - \boldsymbol{r}'|}$ and performing integration by parts with respect to $\boldsymbol{r}$ and $\boldsymbol{r}'$ (the surface term vanishes because the molecular wavefunctions decay exponentially at large distances from the molecule), we obtain

$$V^{(A,B)}_{ab,cd} = \int \mathrm{d}^3r \int \mathrm{d}^3r'\, \nabla_{\boldsymbol{r}} \cdot \boldsymbol{d}^{(A)}_{ab}(\boldsymbol{r})\, \frac{1}{|\boldsymbol{r} - \boldsymbol{r}'|} \nabla_{\boldsymbol{r}'} \cdot \boldsymbol{d}^{(B)}_{cd}(\boldsymbol{r}'), \tag{D1}$$

where for better readability, we have taken real transition dipole densities (otherwise, $\boldsymbol{d}^{(A)}$ would be complex conjugate). With the relation in Eq. (8), we can write this expression in terms of the transition current density,

$$V_{ab,cd}^{(A,B)} = -\int \mathrm{d}^3 r \int \mathrm{d}^3 r' \, \frac{\nabla_{\boldsymbol{r}} \cdot \boldsymbol{j}_{ab}^{(A)}(\boldsymbol{r})}{\omega_{ab}} \, \frac{1}{|\boldsymbol{r}-\boldsymbol{r}'|} \, \frac{\nabla_{\boldsymbol{r}'} \cdot \boldsymbol{j}_{cd}^{(B)}(\boldsymbol{r}')}{\omega_{cd}}. \quad \text{(D2)}$$

Applying Eq. (C1) to both current densities with $\omega_{ab} = E_a - E_b$ and $\omega_{cd} = E_c - E_d$, we finally obtain

$$V_{ab,cd}^{(A,B)} = \int \mathrm{d}^3 r \int \mathrm{d}^3 r' \, \rho_{ab}(\boldsymbol{r}) \, \frac{1}{|\boldsymbol{r}-\boldsymbol{r}'|} \rho_{cd}(\boldsymbol{r}'), \quad \text{(D3)}$$

which is just the definition of $W_{ab,cd}^{(A,B)}$ in Eq. (9).

REFERENCES

[1] H. van Amerongen, L. Valkunas, and R. van Grondelle, *Photosynthetic Excitons* (World Scientific, Singapore, 2000).
[2] M. E. Madjet, A. Abdurahman, and T. Renger, J. Phys. Chem. B **110**, 17268–17281 (2006).
[3] T. Renger and F. Müh, Phys. Chem. Chem. Phys. **15**, 3348 (2013).
[4] T. Brixner, R. Hildner, J. Köhler, C. Lambert, and F. Würthner, Adv. Energy Mater. **7**, 1700236 (2017).
[5] S. K. Saikin, A. Eisfeld, S. Valleau, and A. Aspuru-Guzik, Nanophotonics **2**, 21 (2013).
[6] *J-Aggregates*, edited by T. Kobayashi (World Scientific, 1996).
[7] B. Yang, G. Chen, A. Ghafoor, Y. Zhang, Y. Zhang, Y. Zhang, Y. Luo, J. Yang, V. Sandoghdar, J. Aizpurua, Z. Dong, and J. G. Hou, Nat. Photonics **14**, 693 (2020).
[8] J. Doležal, S. Canola, P. Hapala, R. C. de Campos Ferreira, P. Merino, and M. Švec, ACS Nano **16**, 1082 (2021).
[9] J. Deiglmayr, H. Saßmannshausen, P. Pillet, and F. Merkt, Phys. Rev. Lett. **113**, 193001 (2014).
[10] D. W. Schönleber, A. Eisfeld, M. Genkin, S. Whitlock, and S. Wüster, Phys. Rev. Lett. **114**, 123005 (2015).
[11] A. Browaeys, D. Barredo, and T. Lahaye, J. Phys. B: At., Mol. Opt. Phys. **49**, 152001 (2016).
[12] I. Mourachko, D. Comparat, F. de Tomasi, A. Fioretti, P. Nosbaum, V. M. Akulin, and P. Pillet, Phys. Rev. Lett. **80**, 253 (1998).
[13] V. May and O. Kühn, *Charge and Energy Transfer Dynamics in Molecular Systems*, 3rd ed. (Wiley VCH, 2011).
[14] B. P. Krueger, G. D. Scholes, and G. R. Fleming, J. Phys. Chem. B **102**, 5378 (1998).
[15] L. A. Nafie, J. Chem. Phys. **79**, 4950 (1983).
[16] T. B. Freedman, X. Gao, M.-L. Shih, and L. A. Nafie, J. Phys. Chem. A **102**, 3352–3357 (1998).
[17] G. Hermann, V. Pohl, J. C. Tremblay, B. Paulus, H.-C. Hege, and A. Schild, J. Comput. Chem. **37**, 1511 (2016).
[18] H. T. Dung, L. Knöll, and D.-G. Welsch, Phys. Rev. A **65**, 043813 (2002).
[19] A. Karnieli, N. Rivera, V. Di Giulio, A. Arie, F. J. García de Abajo, and I. Kaminer, Appl. Phys. Rev. **11**, 031305 (2024).
[20] V. Agranovich, Sov. Phys. JETP **10**, 307 (1960).
[21] F. M. Loxsom, J. Chem. Phys. **51**, 4899 (1969).
[22] M.-W. Lee and L.-Y. Hsu, Phys. Rev. A **107**, 053709 (2023).
[23] D. R. Bates and A. Damgaard, Philos. Trans. R. Soc. A **242**, 101 (1949).
[24] A. F. Starace, Phys. Rev. A **3**, 1242 (1971).
[25] C. A. Nicolaides and D. R. Beck, Chem. Phys. Lett. **35**, 202 (1975).
[26] F. Plasser, J. Comput. Chem. **46**, e70072 (2025).
[27] P. J. Lestrange, F. Egidi, and X. Li, J. Chem. Phys. **143**, 234103 (2015).
[28] H. Fidder, J. Knoester, and D. A. Wiersma, J. Chem. Phys. **95**, 7880 (1991).
[29] J. Megow, M. I. S. Röhr, M. Schmidt am Busch, T. Renger, R. Mitrić, S. Kirstein, J. P. Rabe, and V. May, Phys. Chem. Chem. Phys. **17**, 6741 (2015).
[30] C. Weiss, J. Mol. Spectrosc. **44**, 37 (1972).
[31] J. C. Chang, J. Chem. Phys. **67**, 3901 (1977).
[32] V. Czikklely, H. D. Forsterling, and H. Kuhn, Chem. Phys. Lett. **6**, 207 (1970).
[33] L. Gisslén and R. Scholz, Phys. Rev. B **80**, 115309 (2009).
[34] M. Schneider, E. Umbach, and M. Sokolowski, Chem. Phys. **325**, 185 (2006).
[35] H. Huang, S. Chen, X. Gao, W. Chen, and A. T. S. Wee, ACS Nano **3**, 3431 (2009).
[36] A. Stiebeiner, O. Rehband, R. Garcia-Fernandez, and A. Rauschenbeutel, Opt. Express **17**, 21704 (2009).
[37] H. Proehl, R. Nitsche, T. Dienel, K. Leo, and T. Fritz, Phys. Rev. B **71**, 165207 (2005).
[38] E. I. Haskal, Z. Shen, P. E. Burrows, and S. R. Forrest, Phys. Rev. B **51**, 4449 (1995).
[39] Z. G. Soos, M. H. Hennessy, and V. Bulovic, MRS Proc. **598**, 82 (1999).
[40] J. Roden, A. Eisfeld, M. Dvořák, O. Bünermann, and F. Stienkemeier, J. Chem. Phys. **134**, 054907 (2011).
[41] N. Nicoara, J. Gómez-Rodríguez, and J. Méndez, Phys. Status Solidi B **256**, 1800333 (2019).
[42] E. Le Moal, M. Müller, O. Bauer, and M. Sokolowski, Phys. Rev. B **82**, 045301 (2010).
[43] A. Eisfeld, C. Marquardt, A. Paulheim, and M. Sokolowski, Phys. Rev. Lett. **119**, 097402 (2017).
[44] V. Pohl, G. Hermann, and J. C. Tremblay, J. Comput. Chem. **38**, 1515 (2017).
[45] H. F. Arnoldus, J. Mod. Opt. **50**, 755 (2003).
[46] D. G. A. Smith, L. A. Burns, A. C. Simmonett, R. M. Parrish, M. C. Schieber, R. Galvelis, P. Kraus, H. Kruse, R. Di Remigio, A. Alenaizan, A. M. James, S. Lehtola, J. P. Misiewicz, M. Scheurer, R. A. Shaw, J. B. Schriber, Y. Xie, Z. L. Glick, D. A. Sirianni, J. S. O'Brien, J. M. Waldrop, A. Kumar, E. G. Hohenstein, B. P. Pritchard, B. R. Brooks, H. F. Schaefer III, A. Y. Sokolov, K. Patkowski, A. E. DePrince III, U. Bozkaya, R. A. King, F. A. Evangelista, J. M. Turney, T. D. Crawford, and C. D. Sherrill, J. Chem. Phys. **152**, 184108 (2020).
[47] C. D. Sherrill and H. F. Schaefer III, Adv. Quantum Chem. **34**, 143–269 (1999).
[48] J. B. Foresman, M. Head-Gordon, J. A. Pople, and M. J. Frisch, J. Phys. Chem. **96**, 135–149 (1992).
[49] M. J. Frisch, J. A. Pople, and J. S. Binkley, J. Chem. Phys. **80**, 3265 (1984).
[50] M. Wewer and F. Stienkemeier, Phys. Rev. B **67**, 125201 (2003).
[51] M. Müller, A. Paulheim, A. Eisfeld, and M. Sokolowski, J. Chem. Phys. **139**, 044302 (2013).
[52] M. Müller, J. Ikonomov, and M. Sokolowski, Surf. Sci. **605**, 1090–1094 (2011).
[53] J. Krieger and F. Plasser, Chem.-Eur. J. **31**, e01570 (2025).
[54] J. Barnes and P. Hut, Nature **324**, 446 (1986).
[55] U. Saalmann and J. M. Rost, Phys. Rev. Lett. **91**, 223401 (2003).